Materials Advances

ROYAL SOCIETY OF CHEMISTRY

PAPER

View Article Online
View Journal | View Issue

Cite this: *Mater. Adv.*, 2024, 5, 3858

Full Ce substitution on La in Tl_2LaCl_5: impact and performance†

Federico Moretti,* Didier Perrodin, Joanna Szornel and Edith D. Bourret

Received 3rd January 2024,
Accepted 13th March 2024

DOI: 10.1039/d4ma00006d

rsc.li/materials-advances

Scintillators based on Tl salts that provide high densities and high effective atomic numbers are currently being investigated for their possible use in radioisotope identification applications. Ce-doped Tl_2LaCl_5, in particular, has been the leading compound of those studied, showing good light output and energy resolution. The analogous Tl_2CeCl_5 has received much less attention, and the information known about it is rather incomplete. This paper focuses on the scintillation and optical properties of Tl_2CeCl_5 single crystals and compares them to those of Tl_2LaCl_5:Ce to better evaluate the effect of full substitution of La with Ce.

1. Introduction

Scintillating single crystals play a fundamental role in radioisotope identification for Homeland Security applications. Many of the commonly used γ-spectroscopy systems rely on scintillators whose performances are somewhat limited: NaI:Tl, for instance, is fairly bright and very affordable, but it is also characterized by low effective atomic number (Z_{eff}) and density (ρ), as well as by a rather poor energy resolution. More recently developed, commercially available crystals, such as $LaBr_3$:Ce, $CeBr_3$, and SrI_2:Eu have significantly better spectroscopic characteristics with much higher light yields and better energy resolutions. However, they are expensive to manufacture. Furthermore, they still have relatively low Z_{eff} and ρ, and thus do not have significantly improved cross sections for the photoelectric effect. Scintillators with higher Z_{eff} and ρ (*e.g.* $Bi_4Ge_3O_{12}$, Lu_2SiO_5) are available but their performances (particularly in terms of energy resolution and light yield) are not sufficient for γ-spectroscopy applications. Thus, there is a need for materials able to combine high performance, high ρ and Z_{eff}. A possible answer to this need is represented by the relatively recently reported class of Tl-based scintillators in which Tl is a constitutional element of the matrix; Tl is one of the heaviest stable elements in the periodic table and its compounds have high Z_{eff} and ρ.

Tl-based scintillators have been the subject of extensive research, particularly in the past six years, with many possible candidate compositions showing interesting scintillation properties both as intrinsic[1–5] and extrinsic materials.[6–13] The current state of the art has also been recently summarized in a review paper.[14] Tl_2LaCl_5:Ce, among the investigated compositions, appears to be particularly interesting because of its high Z_{eff} and ρ (70 and 5.3 g cm^{-3}, respectively) as well as high light yield (50 000–80 000 photons per MeV), good energy resolution (~3.5% at 663 keV), good non-proportionality, and fast decay times (30–40 ns).[6,7,15,16] The scintillation properties and the decay time, however, strongly depend on the Ce concentration, with the best performances occurring for Ce in the 3–10 mol% concentration range.[15,16]

Although La^{3+} and Ce^{3+} have close ionic radii, Ce segregation phenomena can still occur during the growth of single crystals, leading to non-uniformities in the scintillation properties of the grown crystals. A possible solution to this issue is to consider the complete substitution of La with Ce, thus transitioning from a doped scintillator to an intrinsic one. The resulting Tl_2CeCl_5, however, has received much less attention and only few data on its scintillation and optical properties are present in the literature.[15,17]

In this paper, detailed scintillation and optical properties of Tl_2CeCl_5 single crystals are presented and compared to those of Tl_2LaCl_5: 5 mol% Ce. The measurements include steady state and time-resolved radio- and photoluminescence characterization, as well as pulse height measurements.

2. Materials and methods

$Tl_2La_{1-x}Ce_xCl_5$ single crystals (x = 0.05, 1) were grown in sealed and evacuated quartz ampoules by Bridgman–Stockbarger method starting from stoichiometric mixtures of TlCl, $LaCl_3$, and $CeCl_3$ beads from APL Engineered Materials and EMD Performance Materials. The purity of the raw materials was 99.99% in the case of TlCl and 99.999% for the two rare earth

Lawrence Berkeley National Laboratory, 1 Cyclotron Road Berkeley, CA 94720, USA. E-mail: fmoretti@lbl.gov

† Electronic supplementary information (ESI) available. See DOI: https://doi.org/10.1039/d4ma00006d

chlorides. Due to the hygroscopic nature of both raw materials and synthesized crystals, their handling was performed in Ar-filled glove boxes maintained below 0.1 ppm of O_2 and H_2O. Prior to their sealing, the ampoules were kept under vacuum (10^{-5} mbar) at 110 °C for at least 24 h. The raw materials were fully mixed by melting them several times and inverting the quartz ampules following the procedure reported by Khan *et al.*[16] The crystals were subsequently grown at a rate of 0.5 mm h^{-1}. Pictures of the grown crystals and powder X-ray diffraction characterization are reported in the ESI.† Parts of the obtained crystals were crushed into smaller pieces (0.5–3 mm in each dimension) and put in gas-tight quartz cuvettes for optical characterization.[18]

Room temperature radioluminescence (RL) spectra were collected by exciting the samples with X-rays (50 kVp) generated by a Bruker FR591 rotating anode X-ray tube. The emitted light was collected by a SpectraPro-2150i spectrometer (Acton Research) coupled to a Pixis:1008 CCD detector (Princeton Instruments). All obtained spectra have been corrected for the instrument response. The same light detection system was used for the collection of the photoluminescence excitation (PLE) and emission (PL) maps. In this case, a 75 W Xe lamp and a monochromator (SpectraPro 2150i) were used as an excitation source. Both excitation and emission spectra were corrected for the system response.

A custom built pulsed X-ray system using the time-correlated single photon counting (TCSPC) technique and consisting of a light-excited X-ray tube (Hamamatsu N5084) driven by an ultrafast Ti:sapphire laser (200 fs pulses, Coherent Mira) and a Hamamatsu multichannel plate photomultiplier (R3809U-50) was used to collect scintillation decay measurements. No wavelength discrimination was used to select the light emitted by the samples. The signal is processed through an Ortec 9308 ps analyzer. The overall instrument response function (IRF) of the system has a full width at half maximum (FWHM) of the order of a few hundred ps.[19] The decay times were determined from the experimental results using the method described in Derenzo *et al.*[20]

A Horiba Jobin-Yvon Fluorolog-3 spectrofluorometer working in TCSPC was used to obtain PL decay measurements. The excitation was performed using two different pulsed diodes (NanoLED, Horiba) with emission wavelengths at 268, and 311 nm, each with a FWHM of 10 nm. The system IRF has a 1.6 ns FWHM. Fits of the luminescence decays were performed with Horiba DAS6 software, considering the convolution of the signal with the IRF.

Pulse height spectra were obtained by exciting the samples with a ^{137}Cs γ-ray source (E = 662 keV) with a Hamamatsu R6231-100 photomultiplier (PMT) connected to a Canberra 2005 preamplifier, a Canberra 2022 shaping amplifier and an Ortec EASY-MCA-8K multichannel analyzer. The PMT voltage was set to 700 V. The samples were optically coupled to the PMT window with silicone grease (Viscasil 600000) and covered in several layers of PTFE. The Tl_2LaCl_5:Ce and Tl_2CeCl_5 pieces used in this characterization had dimensions of the order of 3 × 3 × 2 mm^3. The photopeak position and FWHM were evaluated from the obtained spectra by Gaussian fitting, taking into consideration the presence of satellite peaks related to the escape of characteristic X-rays. The absolute number of photons per MeV was estimated by comparing the response of a NaI:Tl (5 × 5 × 2 mm^3) single crystal to those of the $Tl_2La_{1-x}Ce_xCl_5$ samples taking into account the PMT quantum efficiency and the sample RL spectrum. The light output of NaI:Tl was assumed to be 40 000 ph per meV. The non-proportionality of the investigated samples was studied using different radioactive sources.

3. Results

Fig. 1 reports the radioluminescence (RL) spectra of the Tl_2LaCl_5: 5 mol% Ce and Tl_2CeCl_5 samples. The spectrum of the Tl_2LaCl_5:Ce sample is characterized by a bright doublet emission at about 367 and 387 nm, typical of Ce^{3+} 5d to 4f electric dipole allowed interconfigurational transitions. The spectrum is in good agreement with those reported in the literature.[13,15] The short wavelength component is not Gaussian in shape and its amplitude also appears lower than expected, suggesting that the Ce^{3+} emission is affected by self-absorption. In the case of the Tl_2CeCl_5, the spectrum is significantly modified, with the short wavelength component appearing only as a shoulder of the 387 nm band, further reinforcing the hypothesis that self-absorption of the emitted light is indeed a factor in the definition of the Ce^{3+} emission shape. No other emissions are otherwise visible. The obtained spectrum agrees with those reported in the literature.[15,17]

The pulse height spectra of the two investigated samples are reported, with the NaI:Tl reference, in Fig. 2(A). The spectra, obtained by exciting the samples with ^{137}Cs 662 keV photons, show well-defined photopeaks accompanied by the Tl characteristic X-ray escape peak. The energy resolution of Tl_2LaCl_5:Ce sample is significantly higher than that of Tl_2CeCl_5. The

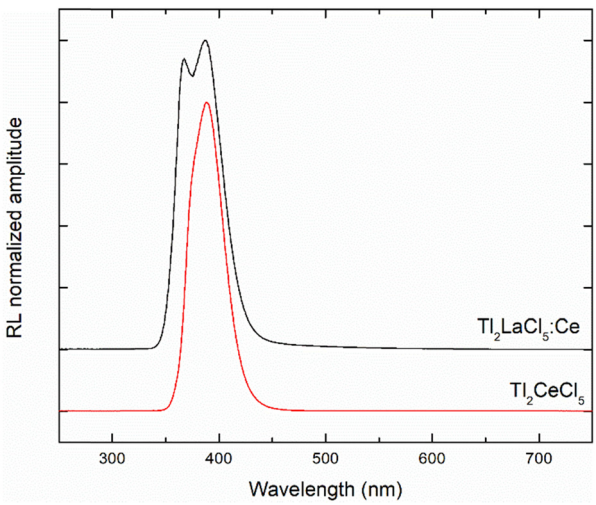

Fig. 1 Normalized room temperature RL spectra of Tl_2LaCl_5: 5 mol% Ce and Tl_2CeCl_5 single crystals. The curves have been shifted along the ordinate axis for clarity.

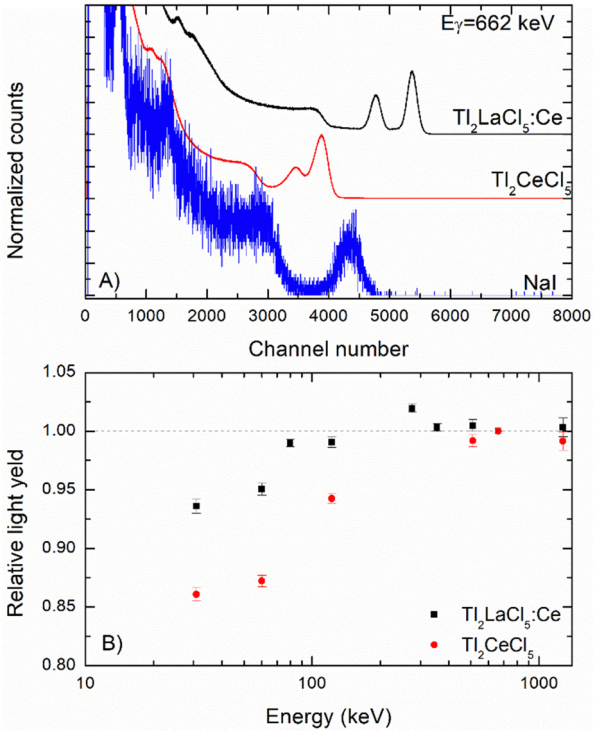

Fig. 2 (A) Normalized pulse height spectra of Tl_2LaCl_5: 5 mol% Ce and Tl_2CeCl_5 single crystals obtained by exciting the samples with a ^{137}Cs 662 keV radioactive source. A spectrum obtained on NaI:Tl in similar experimental conditions is shown for reference. The spectra have been normalized at their photopeak and shifted along the ordinate axis for clarity. (B) Relative light yield of Tl_2LaCl_5: 5 mol% Ce and Tl_2CeCl_5 single crystals as a function of the excitation energy. The data have been obtained from Gaussian fit of photoelectric peaks detected by exciting the samples with different radioactive sources. The data have been normalized at 662 keV.

calculated light yield and energy resolution of the two samples are 51 000 ± 5000 photons per MeV and 3.5% for Tl_2LaCl_5: 5 mol% Ce, and 37 000 ± 3000 photons per MeV and 6.4% for Tl_2CeCl_5. The obtained LY and energy resolution are in relatively good agreement with the literature considering the large spread in reported values.[15,16]

Energy response non-proportionality of the two samples has been studied in order to clarify possible differences that lead to the significantly different light yield and energy resolution. The Tl_2LaCl_5:Ce sample is characterized by a non-proportionality curve with deviations within ~5% in the investigated energy range. On the other hand, the Tl_2CeCl_5 curve has significantly larger deviations, up to 15%, at low gamma-ray energies.

Room temperature pulsed X-ray decays of Tl_2LaCl_5:Ce and Tl_2CeCl_5 samples are presented in Fig. 3. The decays have multiple exponential components for both crystals, with the main decay component of the order of 33 and 27 ns for Tl_2LaCl_5: 5 mol% Ce and Tl_2CeCl_5, respectively, accompanied by longer components. A closer inspection of the decays in the first 300 ns reveals further differences in the decay profile of the two crystals. There is a noticeable 6–7 ns rise time in the case of Tl_2LaCl_5:Ce that is completely absent for the Tl_2CeCl_5 sample. The fully Ce-substituted sample, Tl_2CeCl_5, is characterized by a

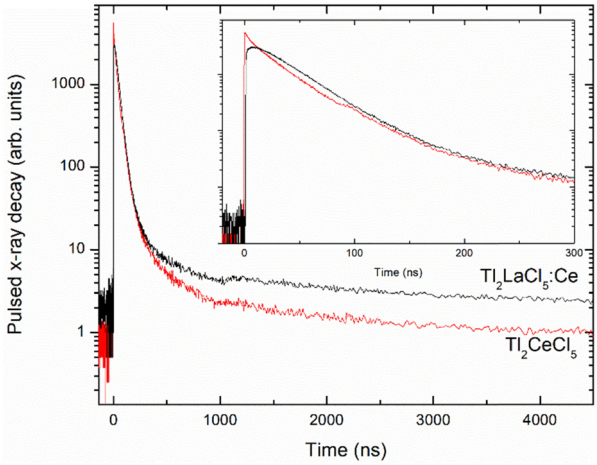

Fig. 3 Room temperature pulsed X-ray decays obtained on Tl_2LaCl_5: 5% Ce and Tl_2LaCl_5 single crystals. The inset is an enlargement of the first 300 ns of the decay profiles. The hump at about 1100 ns is an experimental artifact.

faster decay component of the order of 4 ns, whose nature is not clear at the moment. For both crystals, there are longer minority components of the order of hundreds or thousands of ns likely related to thermal depopulation of defects acting as traps for delocalized carrier. The results of fits performed in terms of multiple exponential decay components of the pulsed X-ray luminescence profiles are reported in Table 1. In both cases, the main component of the pulsed X-ray decays is significantly longer than the expected photoluminescence decay of Ce^{3+} doped samples[21] with emission in the same wavelength range.

Photoluminescence excitation (PLE) and emission (PL) spectra (Fig. 4) were collected to highlight differences in both excitation and emission characteristics of Tl_2LaCl_5: 5 mol% Ce and Tl_2CeCl_5. The PLE spectrum (λ_{em} = 390 nm) of the 5 mol% Ce-doped sample shows two main broad structures, one covering the 200–280 nm region and the second the 290–360 nm wavelength range. The first broad contribution is also visible in the case of undoped Tl_2LaCl_5 samples (not presented),[16] and is likely related to band-to-band transitions of the Tl_2LaCl_5 matrix. The second contribution is related to transitions between 4f and 5d Ce^{3+} levels and it becomes more evident as Ce concentration is increased.[16] The shape of the PLE spectrum is very likely distorted by inner filter effects that

Table 1 Results of fits in terms of 4 exponential decays of the pulsed X-ray profiles reported in Fig. 3. The negative value in the weight of the first decay component for Tl_2LaCl_5: 5 mol% Ce indicates that this contribution is associated with the rise time. The error on the reported decay times is of the order of a few %

	Tl_2LaCl_5: 5 mol% Ce	Tl_2CeCl_5
τ_1 (ns)/A_1 (%)	6.1/−9	3.7/4
τ_2 (ns)/A_2 (%)	33.6/92	27.8/70
τ_3 (ns)/A_3 (%)	143/6	72/19
τ_4 (ns)/A_4 (%)	1760/4	697/3
Const. (%)	7	4

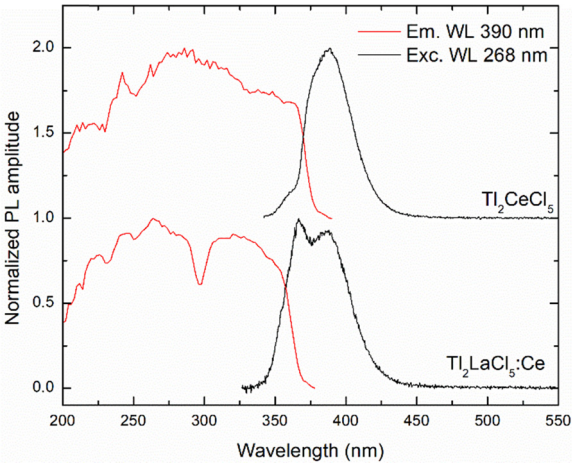

Fig. 4 Room temperature photoluminescence excitation and emission spectra of Tl_2LaCl_5: 5 mol% Ce and Tl_2CeCl_5 single crystals. Excitation and emission wavelengths are reported in the legend.

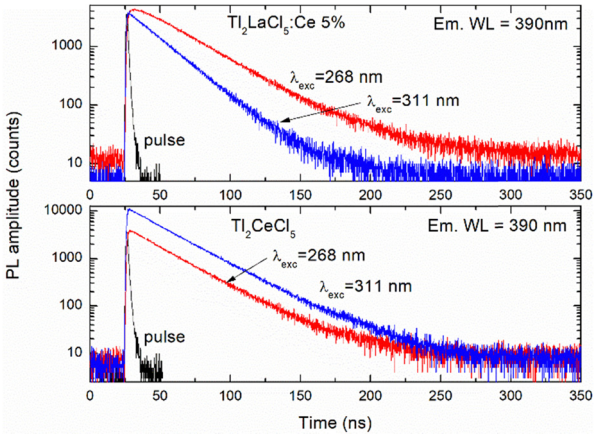

Fig. 5 Room temperature PL decay of Tl_2LaCl_5: 5 mol% Ce (upper panel) and Tl_2LaCl_5 (lower panel) excited at 268 and 311 nm, with emission at 390 nm.

become so predominant to cause the complete loss of any meaningful structure in the PLE detected in the case of Tl_2CeCl_5.

The PL results, obtained with a 268 nm excitation wavelength, which excites the matrix itself, show for both samples very similar spectra to those obtained in RL, though some small variations in shape are visible. In the case of the Tl_2LaCl_5: 5 mol% Ce sample, there is a slight change in the amplitude ratio between the two Ce^{3+} emission components, while in the case of Tl_2CeCl_5, a weak shoulder at about 360 nm is visible. These modifications in the emission spectra can be accounted for by considering a possible less evident role in the reabsorption of the emitted light due to the different excitation volumes obtained with X-rays and 268 nm photons. PL measurements performed at other excitation wavelengths, and notably those at 311 nm, which directly excite the Ce^{3+} electronic transitions, do not show evidence of clear changes in the shape of the Ce^{3+} emission nor the appearance of new luminescence contributions.

PL decay measurements at two excitation wavelengths (268 and 311 nm) with 390 nm as the emission wavelength, were performed to better understand the Ce^{3+} luminescence dynamics and compare it with the pulsed X-ray decays reported above. The results, shown in Fig. 5, show clear differences between the PL decays of the two samples as a function of the excitation wavelength. Tl_2CeCl_5 PL time decays appear practically identical as a function of the excitation wavelength and have a single exponential decay profile. The fit results (reported in Table 2) show that the PL decay times are also very similar to the main decay component obtained with X-ray excitation. On the contrary, the Tl_2LaCl_5: 5 mol% Ce sample is characterized by PL decays that are strongly affected by the excitation wavelength: an evident rise followed by a decay is clearly visible in the case of the 268 nm excitation, while the decay profile appears as a single exponential for the 311 nm excitation. Moreover, the decay following excitation at 311 nm is significantly faster (22 ns) than that obtained with both the X-ray and

Table 2 PL decay fit results obtained by fitting exponential decay components of the data collected from Tl_2LaCl_5: 5 mol% Ce and Tl_2CeCl_5 samples as a function of the excitation wavelength and with 390 nm emission wavelength. The error on the reported decay times is of the order of a few %

Composition	Exc. Wavelength (nm)	τ_1 (ns)/A_1 (%)	τ_2 (ns)/A_2 (%)
Tl_2LaCl_5: 5 mol% Ce	268	6 (−7)	32 (107)
	311	—	22 (100)
Tl_2CeCl_5	268	—	27 (100)
	311	—	28 (100)

268 nm photon (32 ns) excitations. The two latter decays are very similar to each other, excluding the long (hundreds of nanoseconds) components that are visible only for the X-ray excitation and, thus, very likely related to charge carrier trapping phenomena leading to afterglow and scintillation decay tails.

The remarkably different behavior related to the excitation wavelength and the Ce concentration of the two sample luminescence decays suggests that different phenomena are at play in the definition of the scintillation decay dynamics in the Tl_2LaCl_5: 5 mol% Ce and Tl_2CeCl_5 crystals. In particular, the different decay profile detected by exciting within Ce^{3+} transitions clearly suggest that radiative trapping is present in these crystals, and it becomes more pronounced at high Ce concentrations, similarly to what is observed in $LaBr_3$:Ce and $CeBr_3$.[22] This is also in agreement with the substantial change in the shape of the Ce^{3+} luminescence spectrum visible in both PL and RL results. Radiative trapping, however, cannot explain the significant discrepancies observed in the Ce^{3+} decays by exciting the Tl_2LaCl_5: 5 mol% Ce sample at 268 nm or at 310 nm, as well as with X-rays. The clear rise time visible exclusively by exciting the sample with X-rays and 268 nm photons, thus primarily exciting the matrix, suggests that charge carrier diffusion through the matrix and their subsequent transfer to the cerium ions are the limiting processes that determine the

overall cerium luminescence decay. Indeed, undoped Tl_2LaCl_5 is a fairly good scintillator,[13,15] and the centers responsible for its light emission, possibly related to Tl localized states, are involved in the scintillation process even upon Ce doping, thus behaving as competitive channels to the direct charge recombination on the Ce ions. As the cerium concentration is increased, the probability that free charges recombine on Ce also increases at the expense of the slow Tl-related scintillation process. The rather long scintillation decay and the lack of clear matrix-related emission of the 5 mol% Ce doped sample also suggest that the excitation is transferred from these localized states to the Ce ions efficiently, though slowly. The possible competition between Tl and Ce in the scintillation process is being currently investigated, and will be reported on in a separate paper. This explains the very different scintillation decays of Tl_2LaCl_5:Ce reported in the literature as a function of the cerium concentration.[15,16]

4. Conclusions

The scintillation and optical properties of Tl_2CeCl_5 are reported and compared with those of Tl_2LaCl_5: 5 mol% Ce single crystals. Tl_2CeCl_5 shows scintillation with an estimated light yield of the order of 37 000 photons per meV and a fast decay time of 28 ns, but at a relatively poor energy resolution of the order of 6%, compared to 3.5% for Tl_2LaCl_5: 5 mol% Ce single crystal. This poorer energy resolution is related to the substantially less proportional response to γ excitation of Tl_2CeCl_5. Moreover, the significantly higher self-absorption of the emitted light could also affect the overall scintillation characteristics of large Tl_2CeCl_5 single crystals. The obtained results give interesting insights into the scintillation process in the $Tl_2La_{1-x}Ce_xCl_5$ compound family, adding further evidence of the roles of charge carrier migration and radiative trapping in defining the luminescence decay rate of cerium ions.

Conflicts of interest

There are no conflicts to declare.

Acknowledgements

This material is based upon work supported by the Defense Threat Reduction Agency under HDTRA19-31194. This support does not constitute an express or implied endorsement on the part of the United States Government.

References

1 M. Arai, K. Mizoi, Y. Fujimoto, M. Koshimizu, D. Nakauchi, T. Yanagida and K. Asai, *J. Mater. Sci. Mater. Electron.*, 2021, **32**, 7906–7912.
2 M. Arai, Y. Fujimoto, M. Koshimizu, D. Nakauchi, T. Yanagida and K. Asai, *Opt. Mater.*, 2020, **109**, 2–6.
3 G. Rooh, A. Khan, H. J. Kim, H. Park and S. Kim, *Opt. Mater.*, 2017, **73**, 523–526.
4 Y. Fujimoto, M. Koshimizu, T. Yanagida, G. Okada, K. Saeki and K. Asai, *Jpn. J. Appl. Phys.*, 2016, **55**, 3–6.
5 R. Hawrami, E. Ariesanti, H. Wei, J. Finkelstein, J. Glodo and K. S. Shah, *J. Cryst. Growth*, 2017, **475**, 216–219.
6 H. J. Kim, G. Rooh and S. Kim, *J. Lumin.*, 2017, **186**, 219–222.
7 R. Hawrami, E. Ariesanti, H. Wei, J. Finkelstein, J. Glodo and K. S. Shah, *Nucl. Instrum. Methods Phys. Res., Sect. A*, 2017, **869**, 107–109.
8 H. J. Kim, G. Rooh, A. Khan and S. Kim, *Nucl. Instrum. Methods Phys. Res., Sect. A*, 2017, **849**, 72–75.
9 E. van Loef, U. Shirwadkar, L. Soundara Pandian, G. Ciampi, L. Stand, M. H. Du, M. Koschan, M. Loyd, M. Zhuravleva, C. Melcher and K. Shah, *Nucl. Instrum. Methods Phys. Res., Sect. A*, 2021, **995**, 165047.
10 L. Soundara Pandian, M. Loyd, M. H. Du, E. van Loef, G. Ciampi, L. Stand, M. Zhuravleva, M. Koschan, J. Glodo, C. Melcher and K. Shah, *Nucl. Instrum. Methods Phys. Res., Sect. A*, 2021, **988**, 164876.
11 R. Hawrami, E. Ariesanti, L. Soundara Pandian, J. Glodo and K. S. Shah, IEEE Nucl. Sci. Symp. Med. Imaging Conf. (NSS/MIC), 2015 IEEE, 2015, 459, 163–166.
12 R. Hawrami, E. Ariesanti and A. Burger, *J. Cryst. Growth*, 2021, **565**, 126150.
13 A. Khan, P. Quoc Vuong, D. Joseph Daniel, H. J. Kim, G. Rooh and N. T. Luan, *CrystEngComm*, 2022, **24**, 8178–8185.
14 H. Kim, A. Khan, J. Daniel, G. Rooh and P. Q. Vuong, *CrystEngComm*, 2022, **24**, 450–464.
15 U. Shirwadkar, M. Loyd, M. H. Du, E. van Loef, G. Ciampi, L. Soundara Pandian, L. Stand, M. Koschan, M. Zhuravleva, C. Melcher and K. Shah, *Nucl. Instrum. Methods Phys. Res., Sect. A*, 2020, **962**, 163684.
16 A. Khan, P. Q. Vuong, G. Rooh, H. J. Kim and S. Kim, *J. Alloys Compd.*, 2020, **827**, 154366.
17 F. Moretti, D. Onken, D. Perrodin and E. Bourret, *J. Lumin.*, 2022, **241**, 118549.
18 M. Janecek, R. Borade, E. Bourret-Courchesne and S. E. Derenzo, *Nucl. Instrum. Methods Phys. Res., Sect. A*, 2011, **659**, 252–257.
19 S. C. Blankespoor, S. E. Derenzo, W. W. Moses, C. S. Rossington, M. Ito and K. Oba, *IEEE Nucl. Sci. Symp. Rec.*, 1994, **41**, 698–702.
20 S. E. Derenzo, G. A. Bizarri, E. Bourret, R. Borade, Y. Eagleman, G. Gundiah and C. Rosen, *Nucl. Instrum. Methods Phys. Res., Sect. A*, 2018, **908**, 325–332.
21 Y. Pei, X. F. Chen, L. S. Qin, D. M. Yao and G. H. Ren, *Chin. Phys.*, 2006, **15**, 2756–2760.
22 W. Drozdowski, P. Dorenbos, A. J. J. Bos, G. Bizarri, A. Owens and F. G. A. Quarati, *IEEE Trans. Nucl. Sci.*, 2008, **55**, 1391–1396.